**Edelweiss Applied Science and Technology**
*ISSN: 2576-8484*
*Vol. 8, No. 3, 102-124*
*2024*
*Publisher: Learning Gate*
*DOI: 10.55214/25768484.v8i3.1095*


# Kinetic perspectives for the degradation of oxacillin: A penicillanic acid derivative

Yuv Raj Sahu[1], Narendra Kumar Chaudhary[1], Ajaya Bhattarai[1*]
[1]Department of Chemistry, Mahendra Morang Adarsh Multiple Campus, Biratnagar, Tribhuvan University, Nepal; sahuyuvraj09@gmail.com (Y.R.S.), chem_narendra@yahoo.com (N.K.C.), ajaya.bhattarai@mmamc.tu.edu.np (A.B.).

**Abstract:** Oxidation of oxacillin, a penicillanic acid derivative, has been predicted by monoperiodatocuprate [MPC (III)] at 25°C with 0.10 mol $dm^{-3}$ ionic strength, in an aqueous alkaline medium by UV/Visible spectrophotometric analysis, for which 1:4 stoichiometry of oxacillin: MPC (III) is visible. The appearance of a sharp peak by the spectrophotometer confirmed the formation of the complex. The reaction products have been recognized using spectral reports from the FT-IR, LC-MS, melting point, and other spot tests. A pseudo-first-order reaction has been confirmed for the oxidant, fractional order for the substrate, and alkali, even though periodate claimed a delaying effect due to the accumulation of periodate ions from both potassium periodate and monoperiodatocuprate as a common ion effect. The primary active species in the alkaline medium [Cu(H2IO6)(H2O)2] was discovered to be monoperiodatocuprate [MPC (III)]. To figure out the activation and thermodynamic parameters, it is helpful to know the uncatalyzed rate constants, the slow step rate constants, and the equilibrium constants. We have evaluated the dependence of reaction rates on different temperatures. We have calculated rate constants using absorbance data collected from the UV/visible spectrophotometer. We have thoroughly examined the potential rate constant derivation and a plausible mechanism that could explain the experimental findings.

***Keywords:*** *Equilibrium constant, Kinetics, Mechanism, Monoperiodatocuprate (III), Oxacillin, Oxidation.*

## 1. Introduction

β-lactam antibiotics, which are penicillanic acid derivatives (PADs), have been used by humans since the beginning of time to treat bacterial infections. They are widely used in medicine, animal husbandry, nutraceutical products, agriculture, and cosmetics to stop the activity and growth of microbial communities to make our lives better and avoid risks [1]. As a result of these PADs being spread out, excreted, or building up in waste water, sewage plants, hospitals, and industrial effluents, microbes have been developing ways to fight them [2]. Critical evaluation of pharmaceuticals concludes that a majority of PADs are excreted in our urine (55–80%) and feces (4.30%), either alone or in combination with other chemicals that render them inactive [3]. The environmental microbiota of the riverine ecosystem carries out numerous crucial biogeochemical processes, including nutrient cycling and pollutant degradation [4, 5]. Emerging contaminants, or pollutants, are micro-biological pollutants that have the potential to harm humans, flora, and fauna [6]. These contaminants can be harmful to aquatic ecosystems, cause severe infections in people and livestock, and pose a terrible potential threat if misused, overused, transmitted, or dispersed into the environment. Globally deteriorating water quality has overtaken public concern, ecological biodiversity, and even social stability as critical environmental concerns [7]. Prolonged antibiotic exposure can also cause the transfer, proliferation, and diffusion of microbial antibiotic resistance genes (ARGs), as well as the development of "super-resistant bacteria" in the environment or the human body [8]. There are several advanced oxidation processes (AOPs) available, including photo-


**History:** Received: 3 January 2024; Revised: 8 March 2024; Accepted: 15 March 2024; Published: 19 March 2024
* Correspondence: ajaya.bhattarai@mmamc.tu.edu.np

Fenton, stopped-flow, voltammetric oxidation, UV/H2O2, ozonation, and UV/visible spectrophotometry. Researchers continue to investigate the degradation of these PADs in wastewater, organic pollutants, and pharmaceutical waste treatment [9]. On a global scale, organic contaminants are emerging in karst groundwater [10, 11]. Environmental pollution evaluates the occurrence of trace-level antibiotics and personal care products (PPCPs) in Chinese rivers [12, 13]. Similarly, researchers report on the distribution of antibiotic resistance genes in the environment [14] and the processes for removing antibiotics from water and wastewater to safeguard the aquatic environment [15]. We discuss in detail the removal of antibiotics from wastewater and its effects on microbial communities [16]. Water matrix elements, process enhancements, and application influence the removal of antibiotic pollution from wastewater using cutting-edge UV oxidation techniques [17]. Wastewater treatment plant effluent removes pharmaceuticals and antibiotic resistance genes (ARGs), degrades particularly vulnerable free-floating ARGs [18], and facilitates the evolution of antibiotic-resistant bacteria and genes during advanced wastewater treatment and disinfection [19]. Ozone-activated carbon filtering eliminates antibiotic resistance from municipal secondary effluents [19]. Researchers have already examined the impact of water matrix components on the UV/Chlorine process and its response mechanism [20]

Reconstituted penicillins break down in an acidic solution at an elevated temperature to produce penicillanic acid and its derivatives (PADs). Oxacillin, one of the PADs, is a parenteral, 2nd generation semi-synthetic penicillinase-resistant narrow-spectrum penicillin in which the 6-aminopenicillanic acid nucleus consists of a five-membered thiazolidine ring attached to a four-membered beta-lactam ring that responds to antibacterial activities. Oxacillin is a methicillin derivative that has a 5-methyl-3-phenylisoxazole-4-carboxamide group at position 6 β-carbon. It helps fight infections caused by Staphylococcus aureus, which is resistant to penicillin [22]. It is soluble in water (88 mg/ml), ethanol, and dimethylsulfoxide DMSO (< 1 mg/ml) at 298 K. Its formula, molar mass, density, and boiling point are $C_{19}H_{19}N_3O_5S$, 401.44 g $mol^{-1}$, 1.49 g $cm^{-3}$, and 1177.75 K, respectively. Figure 1 outlines the structure of oxacillin.

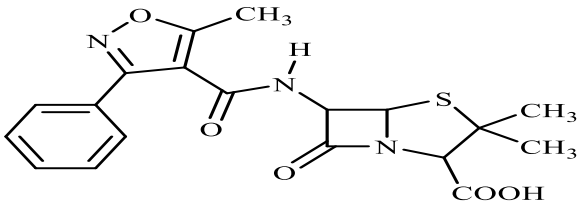


**Figure 1.**
Displays the structure of oxacillin.

Several polydentate ligands, like ditelluratocuprate-III [23, 24] and hexacyanoferrate-III [25], diperiodatocuprate-III [26, 27], diperiodatonickelate-IV [28], and diperiodatoargentate-III [29, 30], can act as strong oxidizing agents to degrade such PADs in the aqueous form. The transition metals of such ligands are capable of forming stable complexes. The properties of DPC (III) were found by studying the kinetics and mechanisms behind the alkaline oxidation of the iodide ion [31]. In aqueous micellar media, alkaline Copper (III) periodate complex synthesis and an analysis of its redox properties have been studied [32]. The geometry of DPC (III) is square planar, and it exhibits a diamagnetic nature and $dsp^2$ hybridization [32, 33]. Cu (III) performs as an active intermediate species between Cu (III)/Cu (II) couple of several electron transfer reactions [34, 35]. Researchers have studied Cobalt (III) complexes as antiviral and antibacterial agents [36].

We evaluated the degradation of oxacillin in water by anodic oxidation with Ti/IrO2 anodes [37]. Ionizing radiation was used to eliminate oxacillin from water, its antibacterial activity, and its toxicity [37]; polyaniline, gold nanourchins, and graphene oxide were molecularly imprinted on screen-printed electrodes to detect oxacillin by voltammetry [38] and heavy metals, their transport, and fate in water, sediment, and some biota were assessed [39]. Likewise, photo-Fenton, electrochemical, and TiO2-

*Edelweiss Applied Science and Technology*
*ISSN: 2576-8484*
*Vol. 8, No. 3: 102-124, 2024*
*DOI: 10.55214/25768484.v8i3.1095*

photocatalysis have been compared for treating oxacillin in water to remove antibiotic activity [40]. Loading penicillin and oxacillin on PEGylated graphene oxide increases the antibiotics' ability to combat methicillin-resistant staphylococcus aureus [41]. Permanganate ion oxidative degradation of some antibiotics in alkaline medium: kinetics and mechanistic [41, 42] and adsorption on water treatment remnants for removing amoxicillin, a member of PADs, from water [43] are discussed.

### *1.1. Significance of the Research*

The diperiodatocupratic (III) oxidation method, which uses this degradation technique, gives the present research significant importance. Hence, the proposed study aims to disclose a novel application in the context of the degradation of non-biodegradable PADs or antibiotics in the aqueous alkaline medium, which may be fruitful in the direction of selecting the best and most rapid ways to reduce pollution and illness problems along with the proper diagnosis of bacterial microorganisms and deactivate their growing potential in the future for the coming generation.

### *1.2. Objectives of the Research*

The purpose of this research is to create a degradation method followed by a UV/Visible spectrophotometry technology and to investigate a plausible mechanism that accounts for activation, thermodynamic characteristics, various rate constants, and the order of the oxidation reaction by examining the kinetics for oxidation of oxacillin by DPC (III) through LC-MS, FT-IR, melting point, and other spot tests through the proper structural and spectral analysis of these complexes and stable products.

## 2. Materials and Methods

### *2.1. Materials*

Potassium hydroxide (KOH), sodium thiosulphate ($Na_2S_2O_3$), potassium persulphate ($K_2S_2O_8$), and potassium iodide (KI) were procured from EMPLURA$^R$ (Merck Life Science, Pvt. Ltd., India). Similarly, potassium nitrate and copper (II) sulphate were procured from LOBA CHEMIE Pvt. Ltd., India, while oxacillin, potassium periodates, and cobalt (III) chloride (hexa-hydrated) were managed by Sigma Aldrich (New Zealand). We used only triple-distilled water throughout the entire research process.

### *2.2. Instruments*

ELICO LI613 pH meter (India) was available for pH measurement. Absorbance readings were noted from the Microprocessor, UV-VIS spectrophotometer with double beam (Model No. 290, Serial No. 1713-2014-03-162, Labtronics, India) with a range of 200-1000 nm. Thermo Nicolet's Avatar 370 FT-IR spectrometer, SHIMADZU Corporation, United States of America, which operates as a KBr disc and has an m/z range of 4000-400 $cm^{-1}$, was used to record the FT-IR spectra of the complexes and their products. LC-MS of the complex and products was captured within the 0–1000 m/z range by using UPLC-TQD Mass Spectrometer (India) in the positive mode.

### *2.3. Synthesis of the Reagent (Oxidant)*

DPC (III) was synthesized by mixing 3.54 g of $CuSO_4$, 6.8 g of $KIO_4$, 2.20 g of $K_2S_2O_8$, and 9.0 g of KOH in a 250 ml round-bottomed (RB) flask [44, 45]. After shaking the mixture frequently, a metal stirrer was used to heat it for nearly 2 hours until the mixture turned intense red followed by possibly removal of extra potassium persulphate. After cooling the dark reddish-brown solution, we used a sintered glass crucible G-4 to filter it and dilute it to 250 ml. DPC (III) was standardized using the thiocyanate method [46] and its concentration was determined. The emergence of an absorption band with its maximum peak at 415 nm confirmed the existence of DPC (III). Possible figures of Diperiodatocuprate or DPC (III), and Monoperiodatocuperate or MPC (III), are depicted in Figure 2.

*Edelweiss Applied Science and Technology*
*ISSN: 2576-8484*
*Vol. 8, No. 3: 102-124, 2024*
*DOI: 10.55214/25768484.v8i3.1095*

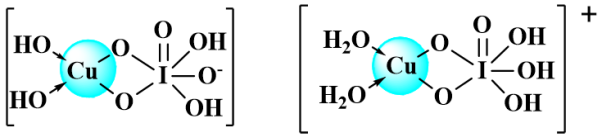


$[Cu(H_2IO_6)(OH)_2]$
**Monoperiodatocuprate**
**MPC (III)**

$[Cu(H_3IO_6)(H_2O)_2]$
**Monoperiodatocuprate**
**MPC (III)**

**Figure 2.**
Displays the possible MPC (III) structures.

*2.4. Synthesis of the Oxacillin- MPC (III) Complex*

The research work was initiated in the UV/Visible spectrophotometer with a double-beam facility. A 100 ml RB flask was filled with 10 ml of standard oxacillin solution (0.132 mol $dm^{-3}$) to conduct the experiment. To this end, standard solutions of 1.0 ml of each $KIO_4$, $KNO_3$, and 2.0 ml of KOH were added in a 1:4 stoichiometric ratio and stirred for 24 hours on a hot plate before continuing to stir during refluxing with condensation. After cooling naturally for three days, we filtered the mixture through Whatman No. 1. While this was going on, $CuSO_4$, the first product added, didn't exhibit any significant interference. Finally, we mixed acrylonitrile in the reaction mixture in the inert atmosphere; the absence of precipitate upon dilution with ethyl alcohol confirmed the absence of any free interfering radical.

*2.5. Kinetic Proceedings*

After 20 minutes of warming up for calibration, the standardized DPC (III) solution was mixed into a quartz cuvette inside the double-beam UV/Visible Spectrophotometer to start the reaction. It was then poured into a fixed volume of oxacillin, which had predetermined standard solutions of $KIO_4$, KOH, and $KNO_3$ to complete the reaction. A UV-Visible spectrophotometer was used to collect data at a wavelength of 415 nm while maintaining a pH of 9.0–9.2 and following the pseudo-first-order suppression order of absorbance at (293.15, 298.15, 303.15, and 308.15) ± 0.2 K, unless otherwise specified. The regression coefficient (r) and standard deviation (s) of the experimental data were calculated using Origin 9.6 (2017) software. Uncatalyzed rate constants ($k_u$) were calculated from slopes after log (abs) versus time plots showed a straight line. Finally, assuming the quantity present in DPC (III) and adding additional amounts allowed us to determine the total concentration of $KIO_4$ and KOH. The reaction composition Table (Table 1) presented herewith shows the effect of changing [DPC (III)], [OXC], [$KIO_4$], and [KOH] to oxidize oxacillin by DPC (III) in the alkaline medium at a temperature of 298 K and 0.10 mol $dm^{-3}$ ionic strength.

**Table 1.**
Displays the reaction composition table.

| (Effect of changing [$KIO_4$], [DPC (III)]*, [KOH] and [OXC] to oxidize oxacillin) | | | | | |
|---|---|---|---|---|---|
| [DPC]x $10^5$ M | [OXC]x $10^4$ M | [KOH]x$10^2$ M | [$KIO_4$]x$10^5$ M | $k_u$x$10^{-4}$($s^{-1}$) | Order |
| 1.0 | 5.0 | 0.12 | 1.0 | 2.41 | ~1 |
| 3.0 | 5.0 | 0.12 | 1.0 | 2.41 | |
| 5.0 | 5.0 | 0.12 | 1.0 | 2.23 | |
| 8.0 | 5.0 | 0.12 | 1.0 | 2.21 | |
| 10.0 | 5.0 | 0.12 | 1.0 | 2.35 | |
| 5.0 | 1.0 | 0.12 | 1.0 | 0.81 | 0.706 |
| 5.0 | 3.0 | 0.12 | 1.0 | 1.14 | |
| 5.0 | 5.0 | 0.12 | 1.0 | 2.23 | |
| 5.0 | 8.0 | 0.12 | 1.0 | 3.48 | |
| 5.0 | 10.0 | 0.12 | 1.0 | 4.15 | |
| 5.0 | 5.0 | 0.04 | 1.0 | 1.02 | 0.562 |
| 5.0 | 5.0 | 0.08 | 1.0 | 1.35 | |
| 5.0 | 5.0 | 0.12 | 1.0 | 2.01 | |

*Edelweiss Applied Science and Technology*
*ISSN: 2576-8484*
*Vol. 8, No. 3: 102-124, 2024*
*DOI: 10.55214/25768484.v8i3.1095*

| (Effect of changing [$KIO_4$], [DPC (III)]*, [KOH] and [OXC] to oxidize oxacillin) | | | | | |
|---|---|---|---|---|---|
| [DPC]x $10^5$ M | [OXC]x $10^4$ M | [KOH]x$10^2$ M | [$KIO_4$]x$10^5$ M | $k_u$ x$10^{-4}$ ($s^{-1}$) | Order |
| 5.0 | 5.0 | 0.16 | 1.0 | 2.23 | |
| 5.0 | 5.0 | 0.20 | 1.0 | 2.35 | |
| 5.0 | 5.0 | 0.12 | 1.0 | 2.23 | |
| 5.0 | 5.0 | 0.12 | 3.0 | 1.84 | -0.265 |
| 5.0 | 5.0 | 0.12 | 5.0 | 1.58 | |
| 5.0 | 5.0 | 0.12 | 8.0 | 1.42 | |
| 5.0 | 5.0 | 0.12 | 10.0 | 1.29 | |

**Note:** *Concentration (Mol $dm^{-3}$) in the bold figure indicates its variation mode.

Scheme 1 illustrates the reaction of oxacillin and diperiodatocuprate (III) in an alkaline medium as follows:

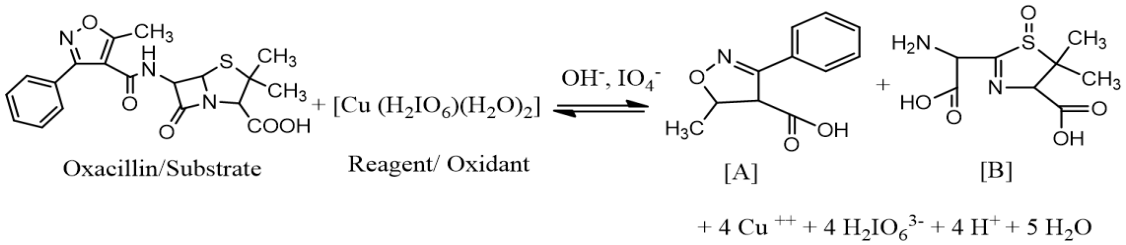


**Scheme 1.**
'A' represents 5-methly-3-phenyl-4,5-dihydroisoxazole-4-carboxyclic acid and 'B' represents 2- (Amino (Carbo) methyl-(5,5)-dimethyl-(4,5)-dihydrothiazole-4-carboxylic acid-1-oxide.

## 3. Results and Discussion

### 3.1. Verification of Beer-Lambert's Law

The complex was cleaned up and re-crystallized in ethanol until only crystals remained after the complete evaporation of the solvent. We observed the maximum absorption peak of the oxidant DPC (III) at 415 nm. Table 2 and Figure 3 represent the absorbance plot against [DPC (III)] to confirm Beer-Lambert's law verification. Similarly, the results from Table 3 indicate a decreasing order of absorbance data collected from the UV/visible spectrophotometer.

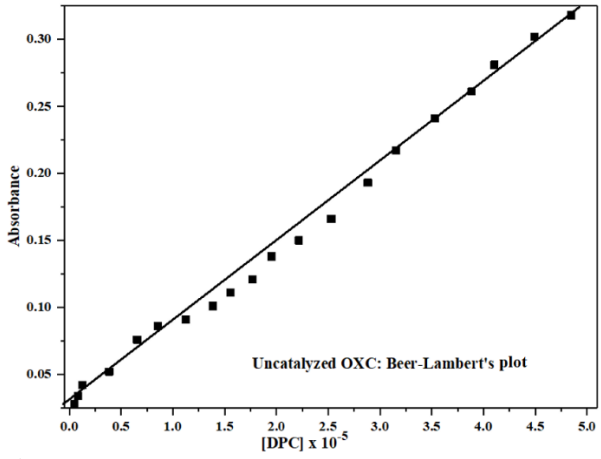


**Figure 3.**
Displays values for the absorbance vs. [DPC (III)] plot.

*Edelweiss Applied Science and Technology*
*ISSN: 2576-8484*
*Vol. 8, No. 3: 102-124, 2024*
*DOI: 10.55214/25768484.v8i3.1095*

**Table 2.**
Displays data for the plot of [DPC (III)] vs. absorbance from UV/Visible spectrophotometer.

| Time in min | Absorbance at 415 nm | [DPC] x $10^{-5}$ M |
|---|---|---|
| 0.0 | 0.318 | 4.845 |
| 0.2 | 0.302 | 4.491 |
| 0.4 | 0.281 | 4.104 |
| 0.6 | 0.261 | 3.885 |
| 0.8 | 0.241 | 3.527 |
| 1.0 | 0.217 | 3.154 |
| 1.2 | 0.193 | 2.883 |
| 1.4 | 0.166 | 2.528 |
| 1.6 | 0.15 | 2.215 |
| 1.8 | 0.138 | 1.952 |
| 2.0 | 0.121 | 1.768 |
| 2.2 | 0.111 | 1.556 |
| 2.4 | 0.101 | 1.385 |
| 2.6 | 0.091 | 1.125 |
| 2.8 | 0.086 | 0.856 |
| 3.0 | 0.076 | 0.654 |
| 3.2 | 0.052 | 0.385 |
| 3.4 | 0.042 | 0.125 |
| 3.6 | 0.034 | 0.085 |
| 3.8 | 0.028 | 0.049 |

*3.2. Reaction Order*

Fresh DPC (III) was diluted between (1.0 x $10^{-5}$ - 1.0 x $10^{-4}$) mol $dm^{-3}$. A plot of time in minutes against log (Absorbance) was linear and nearly parallel, indicating a unit order reaction in DPC (III). Figure 4 and Table 3 confirmed a pseudo-first-order reaction in DPC (III).

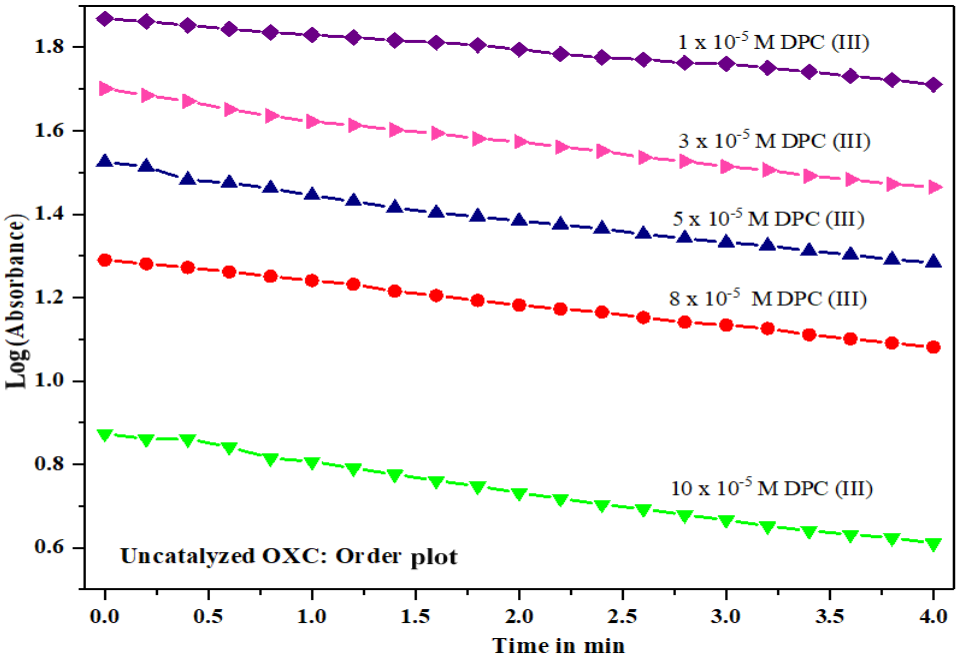


**Figure 4.**
Displays data for the log (Absorbance) vs. time plot.
**Note:** Green, red, blue, pink, and purple lines indicate corresponding concentrations of DPC (III) respectively.

*Edelweiss Applied Science and Technology*
*ISSN: 2576-8484*
*Vol. 8, No. 3: 102-124, 2024*
*DOI: 10.55214/25768484.v8i3.1095*

**Table 3.**
Displays data for order plot for oxidation of PADs (oxacillin) by DPC (III).

| Abs→ Time↓Min | For 1 x $10^{-5}$ M DPC (III) | For 3 x$10^{-5}$ M DPC (III) | For 5 x $10^{-5}$ M DPC (III) | For 8 x $10^{-5}$ M DPC (III) | For 10x $10^{-5}$ M DPC (III) |
|---|---|---|---|---|---|
| 0 | 0.874 | 1.29 | 1.525 | 1.701 | 1.869 |
| 0.2 | 0.861 | 1.281 | 1.514 | 1.685 | 1.862 |
| 0.4 | 0.861 | 1.272 | 1.482 | 1.671 | 1.853 |
| 0.6 | 0.842 | 1.262 | 1.475 | 1.651 | 1.844 |
| 0.8 | 0.815 | 1.251 | 1.462 | 1.636 | 1.836 |
| 1 | 0.807 | 1.241 | 1.445 | 1.622 | 1.83 |
| 1.2 | 0.791 | 1.232 | 1.431 | 1.613 | 1.824 |
| 1.4 | 0.776 | 1.215 | 1.415 | 1.602 | 1.817 |
| 1.6 | 0.761 | 1.205 | 1.403 | 1.594 | 1.812 |
| 1.8 | 0.748 | 1.193 | 1.394 | 1.581 | 1.806 |
| 2 | 0.732 | 1.182 | 1.384 | 1.574 | 1.795 |
| 2.2 | 0.718 | 1.173 | 1.375 | 1.561 | 1.784 |
| 2.4 | 0.704 | 1.165 | 1.365 | 1.552 | 1.776 |
| 2.6 | 0.693 | 1.152 | 1.352 | 1.536 | 1.771 |
| 2.8 | 0.679 | 1.141 | 1.342 | 1.527 | 1.763 |
| 3 | 0.667 | 1.134 | 1.332 | 1.514 | 1.761 |
| 3.2 | 0.652 | 1.126 | 1.325 | 1.506 | 1.751 |
| 3.4 | 0.641 | 1.111 | 1.312 | 1.492 | 1.742 |
| 3.6 | 0.632 | 1.101 | 1.303 | 1.483 | 1.731 |
| 3.8 | 0.624 | 1.091 | 1.291 | 1.472 | 1.722 |
| 4 | 0.611 | 1.081 | 1.284 | 1.465 | 1.711 |

### *3.3. Stoichiometric and Spectral Analysis*

The accurate stoichiometry was confirmed to be 1:4 for OXC: DPC (III) by Job's method [47] after 2.5 hours of storing various batches of reaction mixtures with different DPC (III) to oxacillin ratios in the presence of consistent molarities of KOH and $KNO_3$ in a sealed vessel within $N_2$ atmosphere.

FT-IR and LC-MS spectra are represented in the Appendix as A1 and A2 respectively. Figure A1 declares an absorption peak at 3413.5 $cm^{-1}$ (caused by the carboxylic OH group) [39] and 1276.7 $cm^{-1}$ (caused by the carboxylic C=O group) as well as a peak at 3380.7 $cm^{-1}$ (caused by the N-H stretching) [41] 1464.4 $cm^{-1}$ and 1386.6 $cm^{-1}$ (caused by the geminal $CH_3$ as well as due to stretching mode of (C-N) vibration band [48]1641.2 $cm^{-1}$ (caused by the carboxylic/ketonic C=O group) [48, 49]. Similarly, the complex ($C_{19}H_{25}CuIN_3O_{13}S$) and products were both identified using LC-MS, represented in Figure A2, which produced the first product, $C_{11}H_{11}NO_3$, with a m/z of 204 (m+1) while the second product, $C_8H_{12}N_2O_5S$, showed m/z value at 246 (m+2) respectively.

### *3.4. Effect and Orders of Influencing Factors*

Varying concentrations of DPC (III), OXC, and $KIO_4$ appear as the primary influencing factors, along with their significant effects in the confirmation of the order of reaction. Table 3 and Figure 4 indicate a pseudo-unimolecular reaction with an almost uniformly ordered reaction with respect to DPC (III), which was confirmed by the linearity and parallelism plots of log (absorbance) against time (in minutes). Similarly, the order of oxacillin was declared to be **0.687** ($r \geq 0.999$, $s \leq 0.000014$) after examining within the concentration of (0.0001-0.001) mol $dm^{-3}$; uncatalyzed rate constants ($k_u$) rose up with a rise in the active mass of DPC (III), as illustrated in Figure 5. After investigating the impact of alkali within a molarity range of (0.04 -0.2) mol $dm^{-3}$, the rate constant increased by raising the active mass of alkali (KOH), and the reaction order was ascertained to be **0.562** ($r \geq 0.994$, $s \leq 0.00115$), as confirmed by Figure 6. Meanwhile, the order of reaction for potassium periodate ($KIO_4$) was studied within its active mass between (0.00001- 0.0001) mol $dm^{-3}$ which showed a reaction order of **-0.250** ($r \geq 0.998$, $s \leq 0.00012$) as presented in Figure 7.

*Edelweiss Applied Science and Technology*
*ISSN: 2576-8484*
*Vol. 8, No. 3: 102-124, 2024*
*DOI: 10.55214/25768484.v8i3.1095*

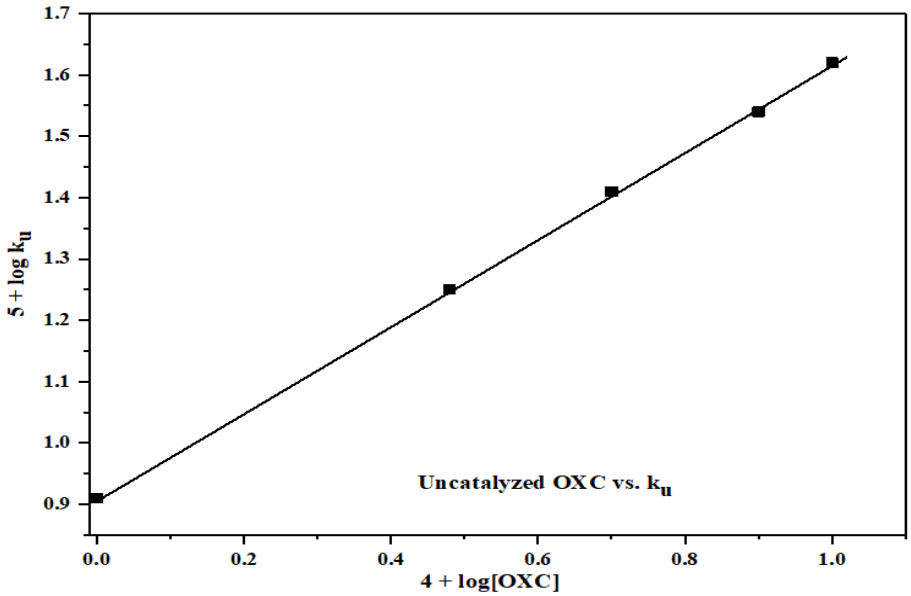


**Figure 5.**
Displays the plot of 4 + log [OXC] vs. (5+ log $k_u$).

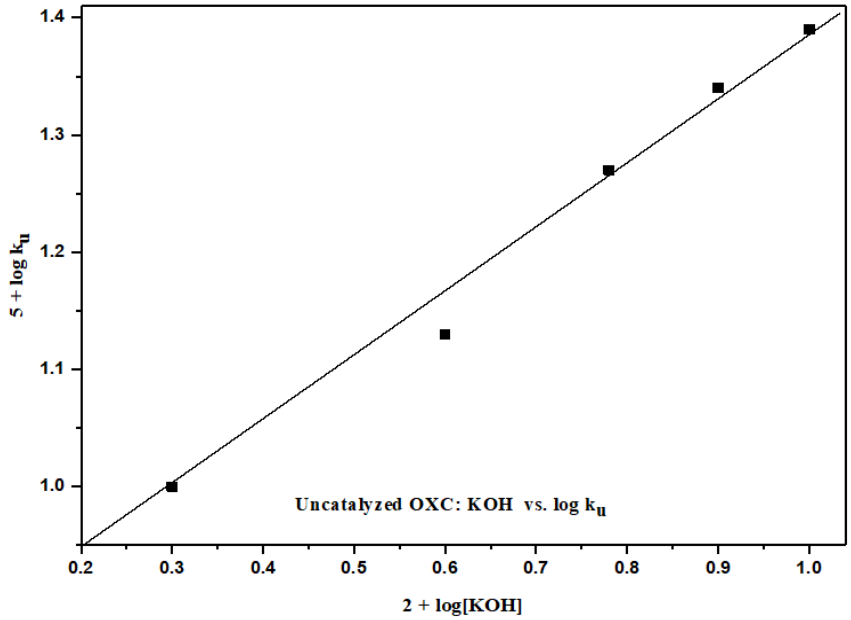


**Figure 6.**
Displays the plot of (5 + log $k_u$) vs. 2 + log [KOH].

*Edelweiss Applied Science and Technology*
*ISSN: 2576-8484*
*Vol. 8, No. 3: 102-124, 2024*
*DOI: 10.55214/25768484.v8i3.1095*

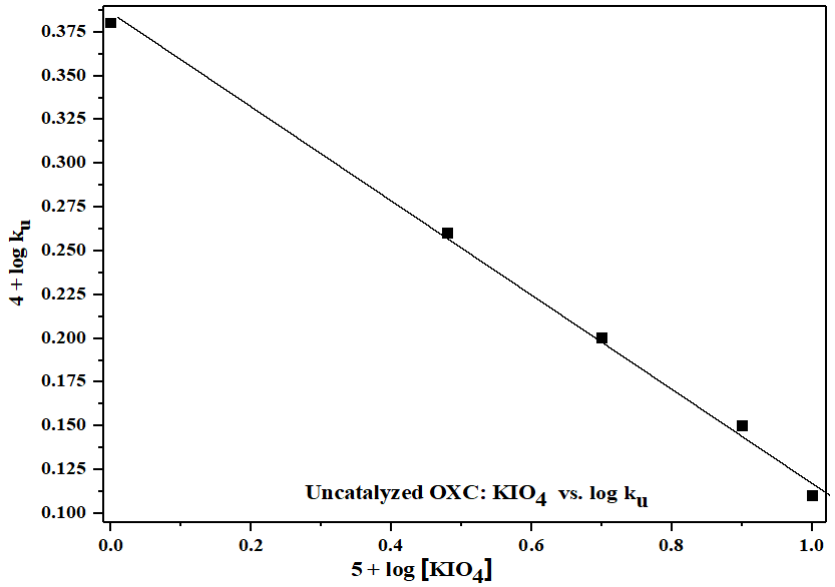


**Figure 7.**
Displays the plot of 5 + log [$KIO_4$] versus (4 + log $k_u$).

*3.5. Effect of Temperature*

Temperature exhibited a significant effect on the order of reaction. While keeping the concentrations of OXC, $KIO_4$, KOH, and DPC (III) constant and varying the other conditions, the effect of temperature on the rate of the oxidation reaction was examined at four different temperatures. The rise in temperature resulted in higher uncatalyzed rate constants in the case of the substrate (oxacillin), oxidizing reagent (DPC-III), and alkali. Only periodate exhibited the retarding effect. With the aid of the Origin 9.6 program, the activation energy and the least square method were used to calculate additional activation parameters. Conducting kinetics in a nitrogen gas atmosphere to examine the impact of periodates, ionic strength, dissolved oxygen, etc. did not reveal any appreciable changes. A plot of (log $k_u$ vs. 1/T) is supported to compute activational parameters due to the uncatalyzed rate constant, represented in Figure 8 and Table 4. Similarly, another plot of the slow step rate constant (k) vs. reciprocal to temperature helped to determine these activation parameters, represented in Figure 9 and Table 5.

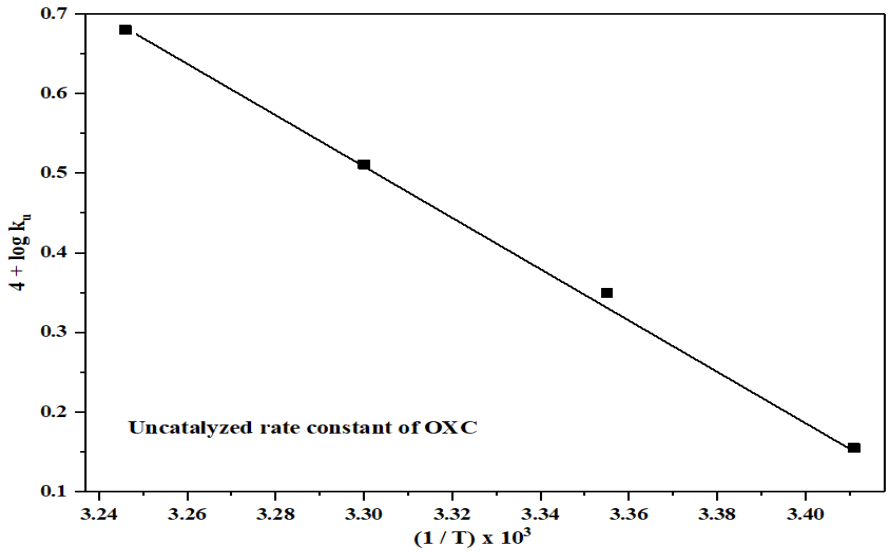


**Figure 8.**

*Edelweiss Applied Science and Technology*
*ISSN: 2576-8484*
*Vol. 8, No. 3: 102-124, 2024*
*DOI: 10.55214/25768484.v8i3.1095*

Displays the plot of (1 / T) x $10^3$ vs. (4 + log $k_u$).

**Table 4.**
Displays activation parameters concerning the uncatalyzed rate constant ($k_u$).

| Activation parameters | Values |
|---|---|
| Ea | 60.44 (kJ $mol^{-1}$) |
| $\Delta H^{\neq}$ | 57 ± 2 (kJ $mol^{-1}$) |
| $\Delta S^{\neq}$ | -101 ± 1 ($JK^{-1}$ $mol^{-1}$) |
| $\Delta G^{\neq}$ | 8 8 ± 2 (kJ $mol^{-1}$) |
| Log A | 6.9 ± 0.2 |

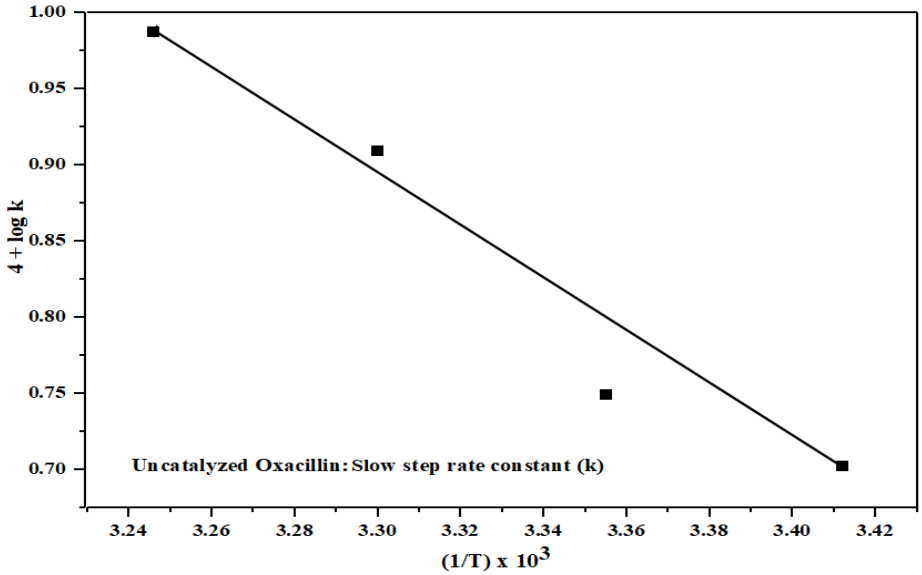


**Figure 9.**
Displays the plot of (1 / T) x$10^3$ versus (4 + log k).

**Table 5.**
Displays activation parameters in relation to the slow step rate constant (k).

| Activation parameters | Values |
|---|---|
| Ea | 35.09 (kJ $mol^{-1}$) |
| $\Delta H^{\neq}$ | 32.6 ± 1 (kJ $mol^{-1}$) |
| $\Delta S^{\neq}$ | -213 ± 2 ($JK^{-1}$ $mol^{-1}$) |
| $\Delta G^{\neq}$ | 98.6 ± 2 (kJ $mol^{-1}$) |
| Log A | 2.4 ± 0.2 |

## 4. Plausible Mechanism

Different β-lactam antibiotics, or PADs, have been subjected to oxidation in the basic medium because DPC (III) functions as both a chelating and an oxidizing agent. Higher alkali concentrations cause the equilibrium forms of periodic acid ($H_5IO_6$) to change into dimerizing $H_4IO_6^{-1}$, $H_3IO_6^{-2}$, and $H_2IO_6^{-3}$ periodate ions. This experimental evidence suggests an appropriate reaction mechanism and the appropriate participation of all reacting species. During the initial phase of the reaction, DPC (III) interacts with the hydroxide ion, producing the deprotonated form of DPC (III). Then, this type of DPC (III) combines with water to produce MPC (III) and free periodate. A new MPC mole (III) and the complex combine to form the intermediate (A). A new mole of MPC (III) and the complex combine to form the intermediate (A). A new mole of MPC (III) and an active intermediate (A) are combined in the following step to produce an intermediate (B), which combines with two more moles of MPC (III) to

*Edelweiss Applied Science and Technology*
*ISSN: 2576-8484*
*Vol. 8, No. 3: 102-124, 2024*
*DOI: 10.55214/25768484.v8i3.1095*

create phenyl-5-methyl-4, 5-dihydroisoxazole-4-carboxylic acid, and 3-(2-(amino (carboxy) methyl)-5, 5-dimethyl-4, 5-dihydrothiazole-4-carboxylic acid-1-oxide, respectively, as mentioned by Scheme 2.

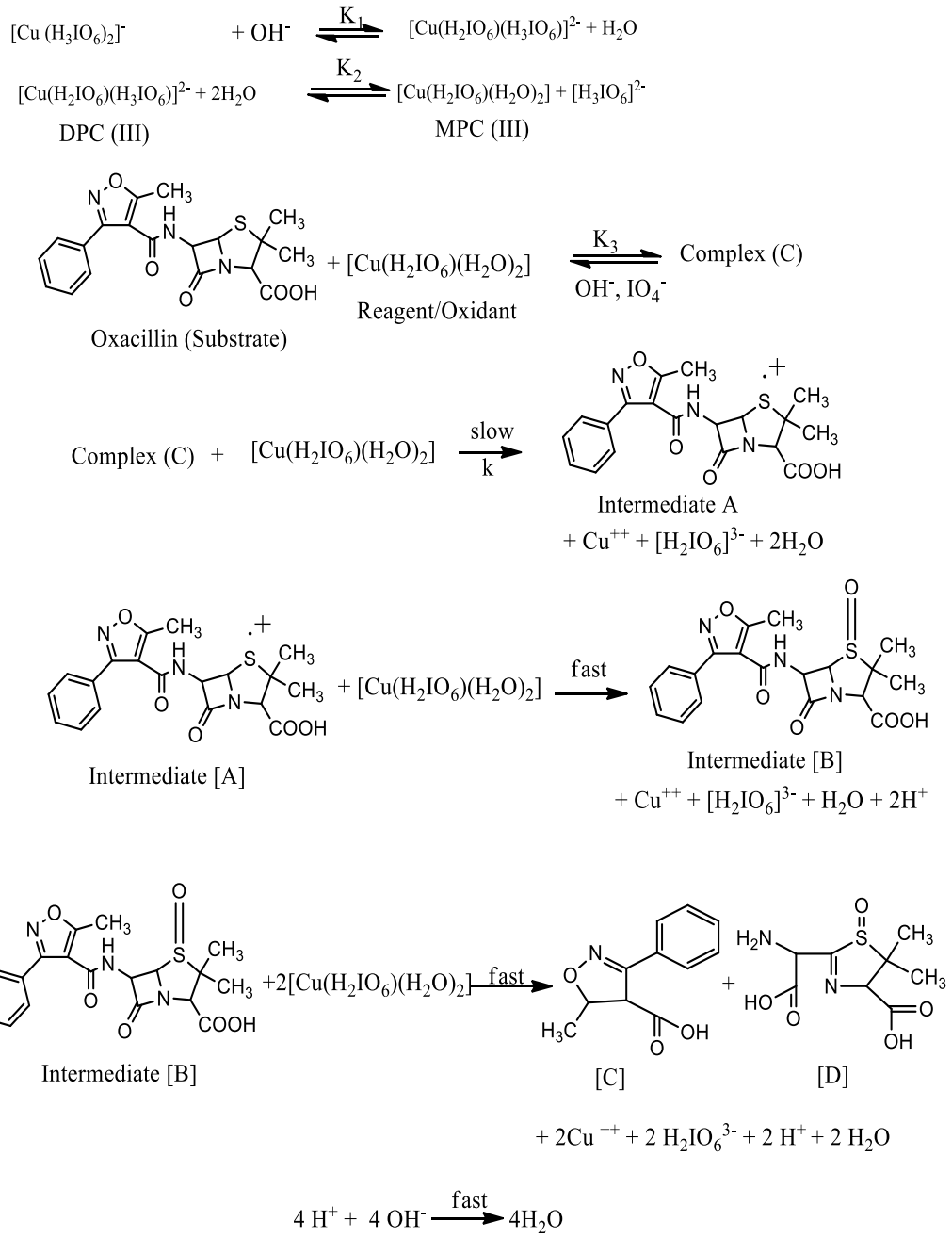


**Scheme 2.**
An elaborate scheme for DPC (III) to oxidize oxacillin.

Figure 10 represents a possible structure for Complex C.

*Edelweiss Applied Science and Technology*
*ISSN: 2576-8484*
*Vol. 8, No. 3: 102-124, 2024*
*DOI: 10.55214/25768484.v8i3.1095*

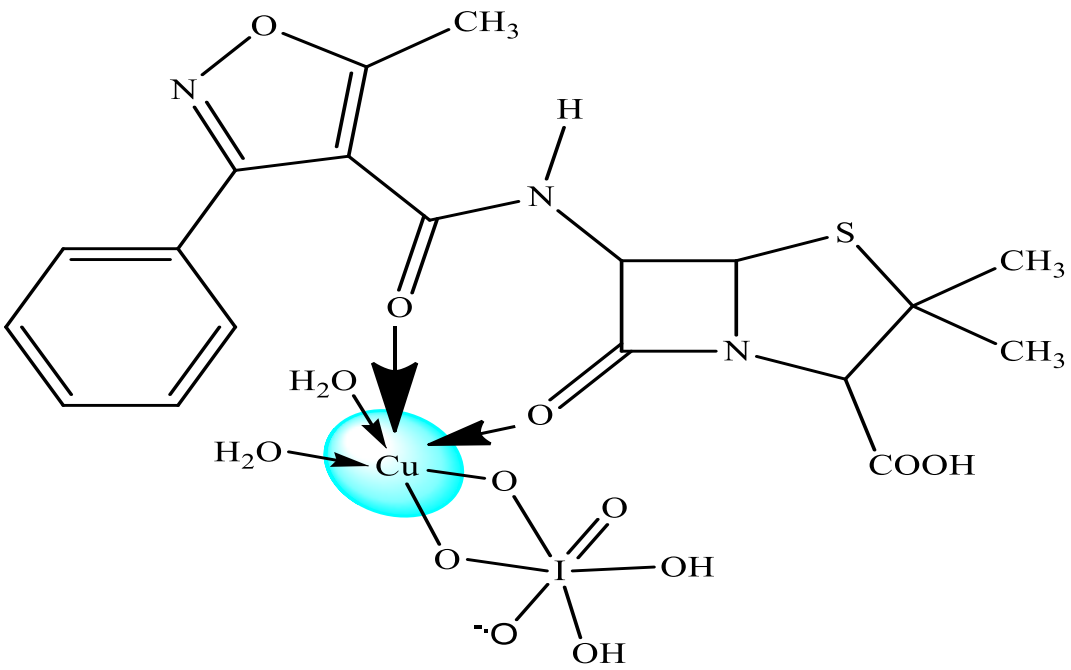


**Figure 10.**
Displays the plausible structure of the complex (C).

The rate law Equation 2 is obtained by Scheme 2 as -

$$\text{Rate} = -\frac{d[DPC]}{dt} = k[C] \qquad [1]$$

$$k_{obs} = \frac{kK_1K_2K_3[DPC][OXC][OH^-]}{[H_3IO_6{}^{2-}]+ K_1[OH^-][H_3IO_6{}^{2-}]+ K_1K_2[OH^-]+K_1K_2K_3[OH^-][OXC]} \qquad [2]$$

All of the observed kinetic orders for various species are described by Equation 2.
Equation 3, suitable for verification, can be created by rearrangement of the rate law Equation 2.

$$\frac{1}{k_{obs}} = \frac{[H_3IO_6{}^{2-}]}{kK_1K_2K_3[OXC][OH^-]} + \frac{[H_3IO_6{}^{2-}]}{kK_2K_3[OXC]} + \frac{1}{kK_3[OXC]} + \frac{1}{k} \qquad [3]$$

The basic equations 5.1 and 5.2 provide the fundamental formula for calculating the activation parameters and the entire rate law derivation, respectively. Finally, verification graphs were reproduced by placing the reciprocal of the uncatalyzed rate constant against the reciprocal of substrate and alkali, while the linearity of periodate was also verified by plotting the reciprocal of the uncatalyzed rate constant against monoperiodatic active masses $[H_2IO_6]^{-3}$. A decrease in the rate of reaction or fractional retarding negative values for periodate may be due to the accumulation of periodate ions, both from DPC (III) as well as from potassium periodate ($KIO_4$) mixed externally in the reaction mixture, which may conduct as common ions. The values of active masses of DPC (III), $KIO_4$, KOH, oxacillin, and slow step rate constants at different temperatures, as well as slopes and intercepts obtained, were utilized to determine equilibrium constants ($K_1$, $K_2$, and $K_3$). The verification or validation plots are displayed in (Figures 11-13) for diperiodatocupratic oxidation of oxacillin. According to Equation 7 the plots of $(1/k_u)$ vs. $1/[OXC]$ ( $r \geq 0.999$, $\leq s\ 0.0042$) (Figure 11), $(1/k_u)$ vs.$1/[KOH]$ ($r \geq 0.999$, $\leq s\ 0.0028$) (Figure 12), and $(1/k_u)$ vs. $[H_2IO_6]^{3-}$ ($r \geq 0.999$, $\leq s\ 0.003$) (Figure 13) are found to be linear. Other plots of equilibrium constants were reproduced by plotting $K_1$, $K_2$ and $K_3$ against reciprocal temperature (Figures 14-16) respectively.

*Edelweiss Applied Science and Technology*
*ISSN: 2576-8484*
*Vol. 8, No. 3: 102-124, 2024*
*DOI: 10.55214/25768484.v8i3.1095*

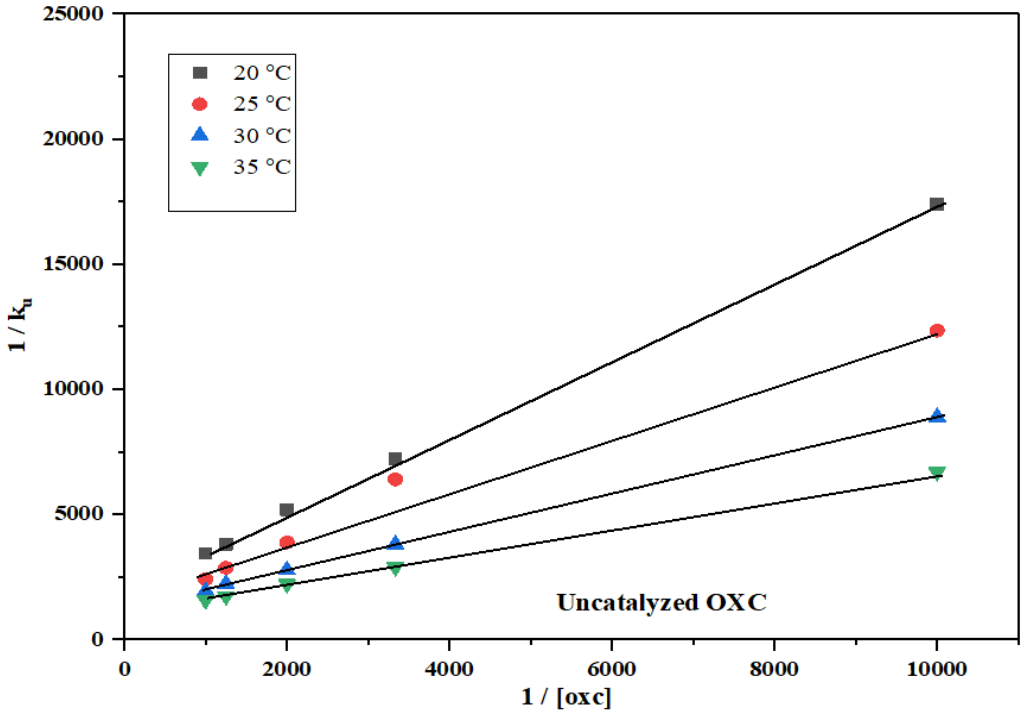


**Figure 11.**
Displays the first verification plot of (1/OXC) vs. $1/k_u$.

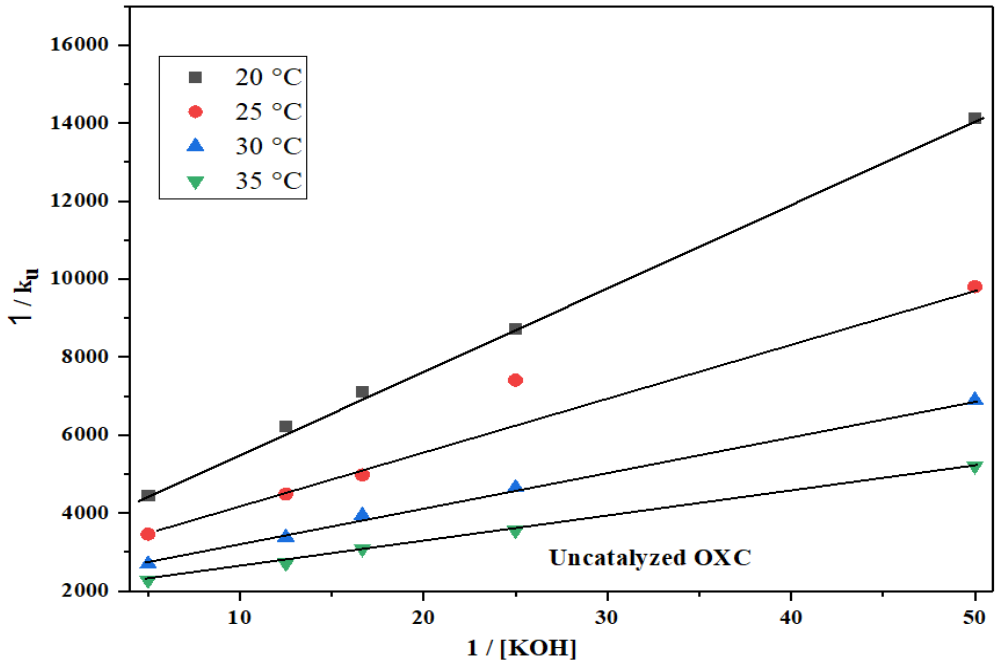


**Figure 12.**
Displays the second verification plot of $1/[KOH]$ vs. $(1/k_u)$.

*Edelweiss Applied Science and Technology*
*ISSN: 2576-8484*
*Vol. 8, No. 3: 102-124, 2024*
*DOI: 10.55214/25768484.v8i3.1095*

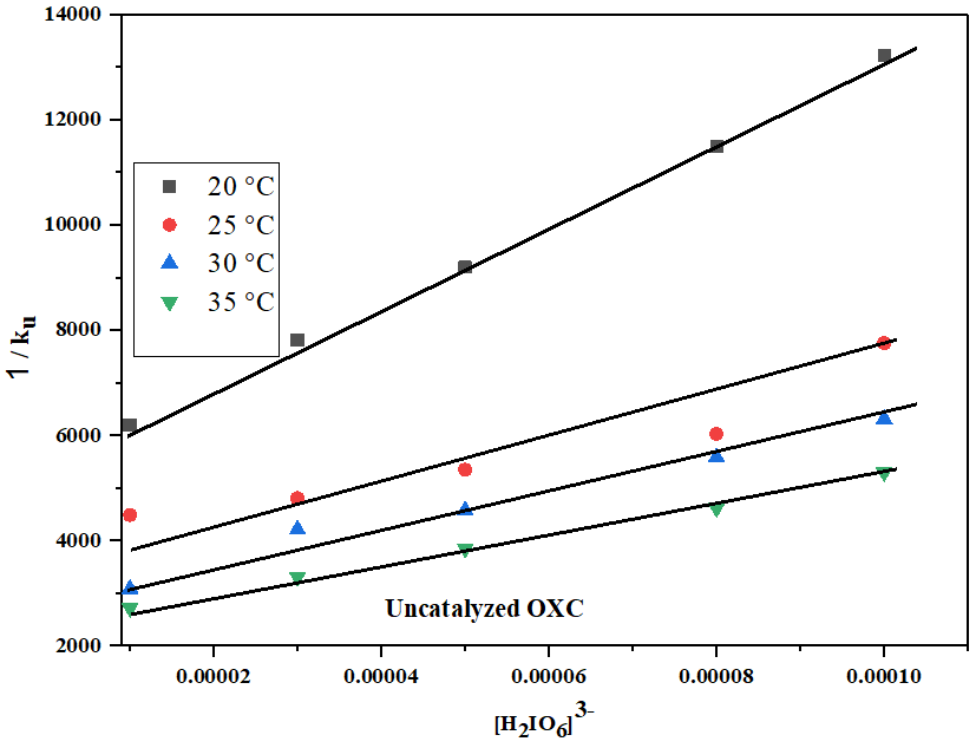


**Figure 13.**
Displays the third verification plot of $(1/k_u)$ vs. $[H_2IO_6]^{3-}$.

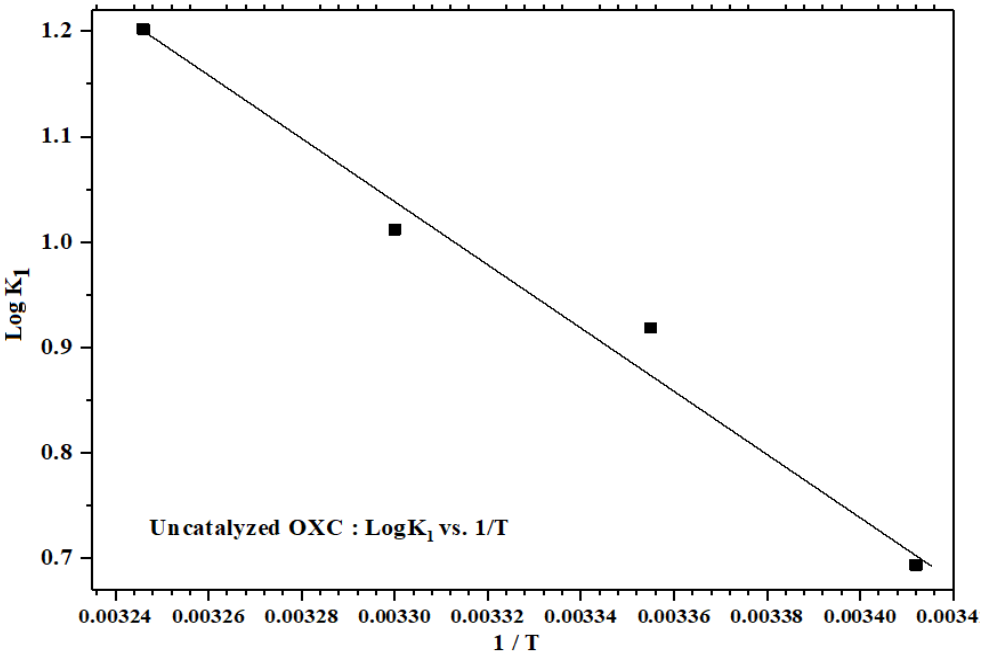


**Figure 14.**
Displays the first equilibrium constant plot of $\log K_1$ vs. $(1/T)$.

*Edelweiss Applied Science and Technology*
*ISSN: 2576-8484*
*Vol. 8, No. 3: 102-124, 2024*
*DOI: 10.55214/25768484.v8i3.1095*

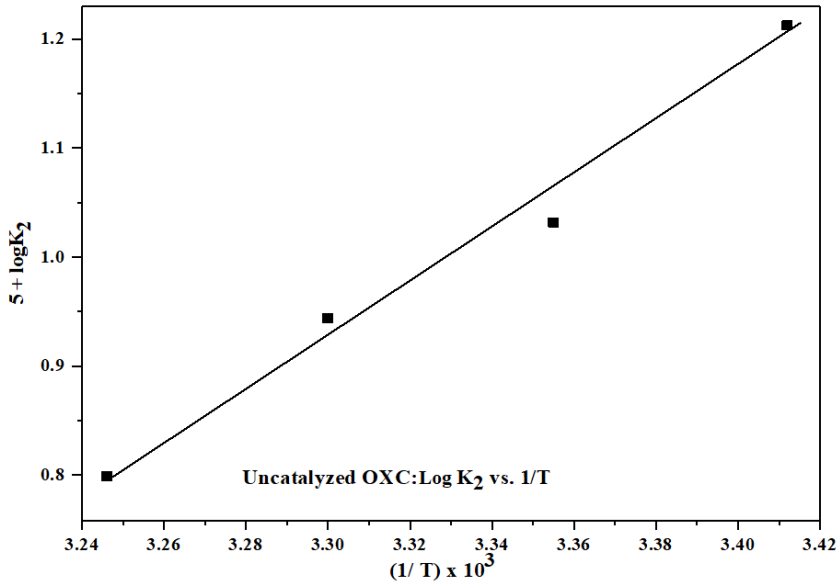


**Figure 15.**
Displays the second equilibrium constant plot of $(5 + \log K_2)$ vs. $(1/T) \times 10^3$.

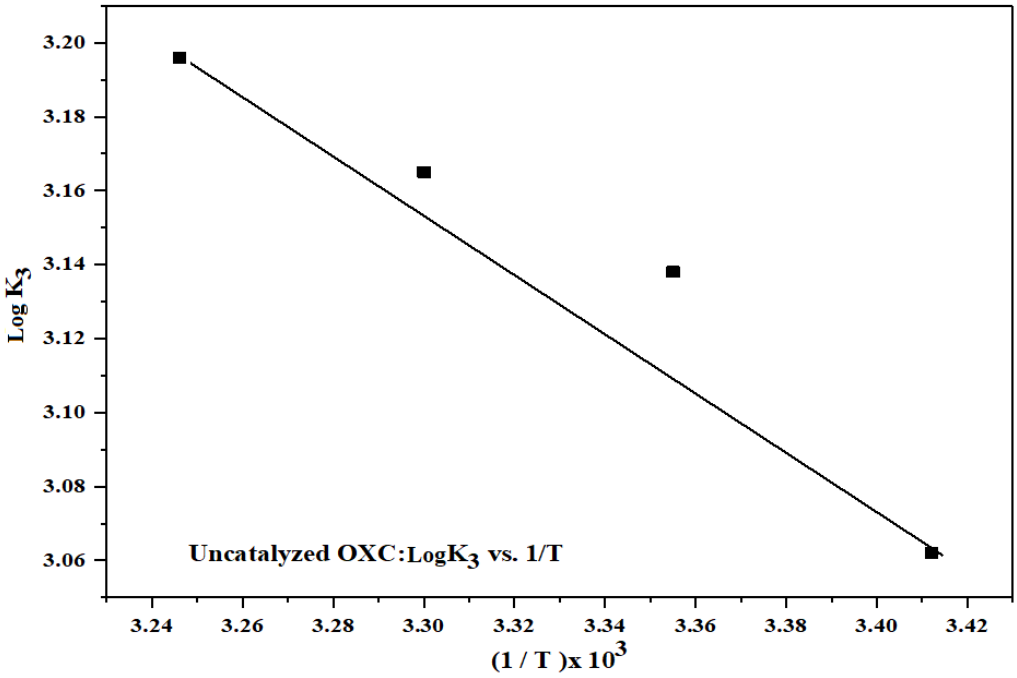


**Figure 16.**
Displays the third equilibrium constant plot of $\log K_3$ vs. $(1/T) \times 10^3$.

Slow step rate constants, equilibrium constants, and various thermodynamic parameters at 298 K are presented in Tables 6 & 7 respectively.

*Edelweiss Applied Science and Technology*
*ISSN: 2576-8484*
*Vol. 8, No. 3: 102-124, 2024*
*DOI: 10.55214/25768484.v8i3.1095*

**Table 6.**
Displays various equilibrium constants and the slow step rate constant.

| **Equilibrium constants ↓** | **Values at variable temperatures** | | | |
|---|---|---|---|---|
| Temperature → | 20 ℃ | 25 ℃ | 30℃ | 35 ℃ |
| k (Slow step rate constant) x $10^{-4}$ | 5.045 | 5.622 | 8.112 | 9.710 |
| $K_1$ | 4.936 | 8.290 | 10.280 | 15.922 |
| $K_2$ x $10^{-4}$ | 1.631 | 1.091 | 0.879 | 0.629 |
| $K_3$ | 1153.453 | 1374.041 | 1462.177 | 1570.362 |

**Table 7.**
Displays thermodynamic parameters from various equilibrium constants at 298 K.

| **Thermodynamic parameters** | **Values (From $K_1$)** | **Values (From $K_2$)** | **Values (From $K_3$)** |
|---|---|---|---|
| $\Delta H^{\circ}_{298}$ (K J $mol^{-1}$) | 56.068 | -11.005 | -3.560 |
| $\Delta S^{\circ}_{298}$ (J $K^{-1}$ $mol^{-1}$) | 204.924 | -32.066 | 26.219 |
| $\Delta G^{\circ}_{298}$ (K J $mol^{-1}$) | - 4.900 | 9.540 | - 7.817 |

## 5. Basic Equations

*5.1. Inter-Conversion of Absorbance into Rate Constant*

The rate constant was calculated from the rate law equation for a first-order reaction as follow:

$$ln(Abs)_t = -k_u t + ln(Abs)_0$$
$$2.303\ log\ (Abs)_t = -k_u t + 2.303\ log\ (Abs)_0$$
$$\text{Or, } k_u\ t = 2.303\ log\ (Abs)_0 - 2.303\ log\ (Abs)_t$$
$$\text{Hence, } k_u = \frac{2.303}{t}\ [log\ (Abs)_0 - log\ (Abs)_t]$$
$$\text{Or, } k_u = \frac{2.303}{t}\ [log\ \frac{(Abs)0}{(Abs)_t}]$$

Here, $k_u$ denotes the uncatalyzed rate constant, $(Abs)_0$ indicates initial absorbance at time '0' sec or just before mixing, and $(Abs)_t$ stands for absorbance at any time sec after mixing all species in the solution phase.

*5.2. Equations for Calculating Activational Parameters*

The activation energy was calculated by,

$$\text{Ea} = -2.303\ \text{R slope}$$

The Arrhenius factor 'A' was calculated by,

$$\text{logA} = \text{log}k_u + \frac{\text{Ea}}{2.303\ \text{RT}}$$

The entropy of activation was determined by,

$$\frac{\Delta S^{\#}}{4.576} = \text{log}k_u - 10.753 - \text{log}T + \frac{E_a}{4.576T}$$

The enthalpy of activation was determined by,

$$\Delta H^{\#} = E_a - RT$$

The free energy of activation was determined by,

$$\Delta G^{\#} = \Delta H^{\#} - T\Delta S^{\#}$$

In the above equations, T denotes the temperature in Kelvin, Ea denotes the activation energy expressed in calories, R denotes the universal gas constant, # denotes the activation parameter, and $k_u/k_{obs}$ denotes the uncatalyzed rate constant expressed in seconds.

*Edelweiss Applied Science and Technology*
*ISSN: 2576-8484*
*Vol. 8, No. 3: 102-124, 2024*
*DOI: 10.55214/25768484.v8i3.1095*

*5.3. Derivation of the Rate Law Equation*

From Scheme 2

$$\text{Rate} = -\frac{d[DPC]}{dt} = k[\text{Complex}] = k[C] \qquad [A\text{-}1]$$

The third equilibrium constant can be calculated using the law of mass action and is given by

$$K_3 = \frac{[C]}{[Cu(H_2IO_6)(H_2O)_2[OXC]}$$

Upon rearrangement,

$$[C] = K_3[Cu(H_2IO_6)(H_2O)_2][OXC] \qquad [A\text{-}2]$$

Replacing the value of C from eqn. [**A-2**]

$$\text{Rate} = -\frac{d[DPC]}{dt} = K_1K_3[Cu(H_2IO_6)(H_2O)_2[OXC] \qquad [A\text{-}3]$$

In the above equation, OXC represents oxacillin.

The second equilibrium constant can be calculated by

$$K_2 = \frac{[Cu(H_2IO_6)(H_2O)_2[H_3IO_6{}^{2-}]}{[Cu(H_2IO_6)(H_3IO_6]^{2-}}$$

This can be rearranged into: -

$$[Cu(H_2IO_6)(H_2O)_2] = \frac{K_2\,[Cu(H_2IO_6)(H_3IO_6]^{2-}}{[H_3IO_6]^{2-}} \qquad [A\text{-}4]$$

The first equilibrium constant can be represented by

$$K_1 = \frac{[Cu(H_2IO_6)(H_3IO_6]^{2-}}{[Cu(H_3IO_6)_2]^{-}[OH^{-}]}$$

This can be rearranged into

$$[Cu(H_2IO_6)(H_3IO_6]^{2-} = K_1\,[Cu(H_3IO_6)_2]^{-}[OH^{-} \qquad [A\text{-}5]$$

Substituting eqn. [**A-4**] to [**A-5**] in eqn. [**A-3**], we get

$$\text{Rate} = -\frac{d[DPC]}{dt} = \frac{kK_1K_2K_3[OXC]_f[DPC]_f[OH^{-}]_f}{[H_3IO_6)_2]^{-}} \qquad [A\text{-}6]$$

The total concentration of [DPC] can be given as

$$[DPC]_T = [DPC]_f + [Cu(H_2IO_6)(H_3IO_6]^{2-} + [Cu(H_2IO_6)(H_2O)_2] + [C] \qquad [A\text{-}7]$$

Where T and f denote total and free concentrations

$$= [DPC]_f + K_1[Cu(H_2IO_6)_2]^{-}[OH^{-}] + \frac{K_1K_2[Cu(H_2IO_6)_2]^{-}[OH^{-}]}{[H_3IO_6{}^{2-}]} + \frac{K_1K_2K_3[Cu(H_3IO_6)_2]^{-}[OH^{-}][OXC]}{[H_3IO_6]^{2-}}$$

$$[DPC]_T = [DPC]_f + K_1[DPC]_f[OH^{-}] + \frac{K_1K_2[DPC]_f[OH^{-}]}{[H_3IO_6{}^{2-}]} + \frac{K_1K_2K_3[DPC]_f[OH^{-}][OXC]}{[H_3IO_6{}^{2-}]}$$

$$[DPC]_f = \frac{[DPC]_T[H_3IO_6{}^{2-}]}{[H_3IO_6{}^{2-}] + K_1[OH^{-}][H_3IO_6{}^{2-}] + K_1K_2[OH^{-}] + K_1K_2K_3[OH^{-}][OXC]} \qquad [A\text{-}8]$$

The total concentration of [OH-] can be given by

*Edelweiss Applied Science and Technology*
*ISSN: 2576-8484*
*Vol. 8, No. 3: 102-124, 2024*
*DOI: 10.55214/25768484.v8i3.1095*

$$[OH^-]_T = [OH^-]_f + [Cu(H_2IO_6)(H_3IO_6]^{2-} + [Cu(H_2IO_6)(H_2O)_2] + [C]$$

$$[OH^-]_T = [OH^-]_f + K_1[DPC][OH^-]_f + \frac{K_1K_2[DPC][OH^-]_f}{[H_3IO_6]^{2-}} + \frac{K_1K_2K_3[DPC][OH^-]_f[OXC]}{[H_3IO_6]^{2-}}$$

$$[OH^-]_T = [OH^-]_f \{1 + K_1[DPC] + \frac{K_1K_2[DPC]}{[H_3IO_6]^{2-}} + \frac{K_1K_2K_3[DPC][OXC]}{[H_3IO_6]^{2-}})$$

Because DPC (III) and $H_3IO_6^{-2}$ were used in such small amounts, these terms can be neglected.

$$[OH^-]_T = [OH^-]_f \qquad [A\text{-}9]$$

Similarly, in the case of low concentrations of DPC (III) and $H_3IO_6^{2-}$ used

$$[OXC]_T = [OXC]_f \qquad [A\text{-}10]$$

Substituting the value of [DPC]$_f$ from eq$^n$. [**A-8**], [OH$^-$]$_f$ from eq$^n$. [**A-9**] and [OXC]$_f$ from eq$^n$. [**A-10**] in eq$^n$. [**A-6**] After omitting subscripts T and f, we get,

$$\text{Rate} = -\frac{d[DPC]}{dt} = \frac{kK_1K_2K_3[OXC][DPC][OH^-]}{[H_3IO_6{}^{2-}] + K_1[OH^-][H_3IO_6{}^{2-}] + K_1K_2[OH^-] + K_1K_2K_3[OH^-][OXC]}$$

$$\text{Or, } \frac{1}{k_{obs}} = \frac{[H_3IO_6{}^{2-}]}{kK_1K_2K_3[OXC][OH^-]} + \frac{[H_3IO_6{}^{2-}]}{k\,K_2K_3[OXC]} + \frac{1}{kK_3[OXC]} + \frac{1}{k} \qquad [A\text{-}11]$$

## 6. Conclusion

MPC (III) is regarded as the main active species, as [Cu ($H_2IO_6$)($H_2O$)$_2$], for the current research work to oxidize oxacillin in an alkaline medium. The mechanism clearly demonstrates the involvement of neutral species because of the constant ionic strength and dielectric constant. The moderate activation entropy and enthalpy values are beneficial for electron transfer reactions, as they are within the range of electron coupling and uncoupling processes, resulting in the loss of a degree of freedom and a rigid transition state. According to the intermediate complex, it is likely to be more highly ordered than the reacting species, according to the intermediate complex's higher negative value of entropy of activation. The aforementioned findings, supporting evidence, and smaller rate constant for slow steps suggest that an inner-sphere mechanism is most likely responsible for oxidation. Lack of a catalyst most likely causes the substrate's reducing ability, while raising the activation energy lengthens the uncatalyzed reaction's pathway. At various temperatures, activation and thermodynamic parameters are calculated and computed concerning equilibrium constants ($K_1$, $K_2$, and $K_3$), uncatalyzed rate constant (ku), and the slow step rate constant (k). The overall sequences presented herein are supported by all available experimental data, including product, spectral, mechanistic, and kinetic studies that establish the pseudo-unimolecular nature of oxacillin oxidation in the alkaline medium.

## Funding:

This study received no specific financial support.

## Institutional Review Board Statement:

Not applicable.

## Transparency:

The authors confirm that the manuscript is an honest, accurate, and transparent account of the study; that no vital features of the study have been omitted; and that any discrepancies from the study as planned have been explained. This study followed all ethical practices during writing.

*Edelweiss Applied Science and Technology*
*ISSN: 2576-8484*
*Vol. 8, No. 3: 102-124, 2024*
*DOI: 10.55214/25768484.v8i3.1095*

## Competing Interests:
The authors declare that they have no competing interests.

## Authors' Contributions:
All authors contributed equally to the conception and design of the study. All authors have read and agreed to the published version of the manuscript.



## References
[1] J. Wang, S. Xu, K. Zhao, G. Song, S. Zhao, and R. Liu, "Risk control of antibiotics, antibiotic resistance genes (ARGs) and antibiotic resistant bacteria (ARB) during sewage sludge treatment and disposal: A review," *Science of The Total Environment*, vol. 877, p. 162772, 2023. https://doi.org/10.1016/j.scitotenv.2023.162772

[2] X. Guo, C. Feng, E. Gu, C. Tian, and Z. Shen, "Spatial distribution, source apportionment and risk assessment of antibiotics in the surface water and sediments of the Yangtze Estuary," *Science of the Total Environment*, vol. 671, pp. 548-557, 2019. https://doi.org/10.1016/j.scitotenv.2019.03.393.

[3] S. R. Hughes, P. Kay, and L. E. Brown, "Global synthesis and critical evaluation of pharmaceutical data sets collected from river systems," *Environmental Science & Technology*, vol. 47, no. 2, pp. 661-677, 2013. https://doi.org/10.1021/es3030148

[4] B. I. Escher, R. Baumgartner, M. Koller, K. Treyer, J. Lienert, and C. S. McArdell, "Environmental toxicology and risk assessment of pharmaceuticals from hospital wastewater," *Water Research*, vol. 45, no. 1, pp. 75-92, 2011. https://doi.org/10.1016/j.watres.2010.08.019.

[5] Y. Guan and Z. Wang, "Analysis of bacterial community characteristics, abundance of antibiotics and antibiotic resistance genes along a pollution gradient of Ba River in Xi'an, China," *Frontiers in Microbiology*, vol. 9, p. 415188, 2018. https://doi.org/10.3389/fmicb.2018.03191.

[6] I. C. Vasilachi, D. M. Asiminicesei, D. I. Fertu, and M. Gavrilescu, "Occurrence and fate of emerging pollutants in water environment and options for their removal," *Water*, vol. 13, no. 2, p. 181, 2021. https://doi.org/10.3390/w13020181

[7] C. J. Vörösmarty *et al.*, "Global threats to human water security and river biodiversity," *Nature*, vol. 467, no. 7315, pp. 555-561, 2010. https://doi.org/10.1038/nature09440

[8] J. L. Martínez, T. M. Coque, and F. Baquero, "What is a resistance gene? Ranking risk in resistomes," *Nature Reviews Microbiology*, vol. 13, no. 2, pp. 116-123, 2015. https://doi.org/10.1038/nrmicro3399

[9] P. K. Pandis *et al.*, "Key points of advanced oxidation processes (AOPs) for wastewater, organic pollutants and pharmaceutical waste treatment: A mini review," *Chem Engineering*, vol. 6, no. 1, p. 8, 2022. https://doi.org/10.3390/chemengineering6010008

[10] J. L. Reberski, J. Terzić, L. D. Maurice, and D. J. Lapworth, "Emerging organic contaminants in karst groundwater: A global level assessment," *Journal of Hydrology*, vol. 604, p. 127242, 2022. https://doi.org/10.1016/j.jhydrol.2021.127242

[11] S. Xiang *et al.*, "Response of microbial communities of karst river water to antibiotics and microbial source tracking for antibiotics," *Science of the Total Environment*, vol. 706, p. 135730, 2020. https://doi.org/10.1016/j.scitotenv.2019.135730

[12] T. Z. Addis, J. T. Adu, M. Kumarasamy, and M. Demlie, "Occurrence of trace-level antibiotics in the Msunduzi River: An investigation into South African environmental pollution," *Antibiotics*, vol. 13, no. 2, p. 174, 2024. https://doi.org/10.3390/antibiotics13020174

[13] J.-L. Liu and M.-H. Wong, "Pharmaceuticals and personal care products (PPCPs): A review on environmental contamination in China," *Environment International*, vol. 59, pp. 208-224, 2013. https://doi.org/10.1016/j.envint.2013.06.012

[14] M. Zhuang *et al.*, "Distribution of antibiotic resistance genes in the environment," *Environmental Pollution*, vol. 285, p. 117402, 2021. https://doi.org/10.1016/j.envpol.2021.117402

[15] M. S. De Ilurdoz, J. J. Sadhwani, and J. V. Reboso, "Antibiotic removal processes from water & wastewater for the protection of the aquatic environment-a review," *Journal of Water Process Engineering*, vol. 45, p. 102474, 2022. https://doi.org/10.1016/j.jwpe.2021.102474.

[16] M. Hassan *et al.*, "Removal of antibiotics from wastewater and its problematic effects on microbial communities by bioelectrochemical Technology: Current knowledge and future perspectives," *Environmental Engineering Research*, vol. 26, no. 1, 2021. https://doi.org/10.4491/eer.2019.405

[17] Y. Zhang, Y.-G. Zhao, F. Maqbool, and Y. Hu, "Removal of antibiotics pollutants in wastewater by UV-based advanced oxidation processes: Influence of water matrix components, processes optimization and application: A review," *Journal of Water Process Engineering*, vol. 45, p. 102496, 2022. https://doi.org/10.1016/j.jwpe.2021.102496.

[18] S. Gajdoš *et al.*, "Synergistic removal of pharmaceuticals and antibiotic resistance from ultrafiltered WWTP effluent: Free-floating ARGs exceptionally susceptible to degradation," *Journal of Environmental Management*, vol. 340, p. 117861, 2023. https://doi.org/10.1016/j.jenvman.2023.117861

[19] T. Spit, J. P. van der Hoek, C. de Jong, D. van Halem, M. de Kreuk, and B. B. Perez, "Removal of antibiotic resistance from municipal secondary effluents by ozone-activated carbon filtration," *Frontiers in Environmental Science*, vol. 10, p. 834577, 2022. https://doi.org/10.3389/fenvs.2022.834577

[20] I. Velo-Gala, M. J. Farré, J. Radjenovic, and W. Gernjak, "Influence of water matrix components on the UV/chlorine process and its reactions mechanism," *Environmental Research*, vol. 218, p. 114945, 2023. https://doi.org/10.1016/j.envres.2022.114945

[21] Y. R. Sahu, R. K. Dev, N. K. Chaudhary, and A. Bhattarai, "Kinetics of catalytic oxidation of carbenicillin: A degradation approach for penicillanic acid derivatives (PADs)," *Journal of Nepal Chemical Society*, vol. 43, no. 2, pp. 159-170, 2023.

[22] P. Krupa, J. Bystroń, M. Podkowik, J. Empel, A. Mroczkowska, and J. Bania, "Population structure and oxacillin resistance of Staphylococcus aureus from pigs and pork meat in South-West of Poland," *BioMed Research International*, vol. 2015, pp. 1-10, 2015. https://dx.doi.org/10.1155/2015/141475

[23] J.-h. Shan, Y. Li, S.-y. Huo, and C.-h. Yin, "The oxidation of 2-(2-methoxyethoxy) ethanol and 2-(2-ethoxyethoxy) ethanol by ditelluratocuprate (III): A kinetic and mechanistic study," *Journal of Chemistry*, vol. 2013, pp. 1-6, 2013. https://doi.org/10.1155/2013/627324

[24] J. Shan, Y. Liu, and J. Zhang, "Kinetics and mechanism of oxidation of 1-methoxy-2-propanol and 1-ethoxy-2-propanol by ditelluratocuprate (III) in alkaline medium," *Chinese Journal of Chemistry*, vol. 29, no. 4, pp. 639-642, 2011. https://doi.org/10.1002/cjoc.201190134

[25] I. A. Amer, "Kinetics and mechanism of the oxidation of 2-methylindole by alkaline potassium hexacyanoferrate (III)," *Egyptian Journal of Chemistry*, vol. 64, no. 3, pp. 1441-1446, 2021. https://doi.org/10.21608/ejchem.2020.22459.2338

[26] M. Thriveni, I. Mallikarjuna, S. Bellappa, and T. Shivalingaswamy, "Oxidation of caffeine by Diperiodatocuprate (III) with and without Ruthenium (III) in alkaline medium," *Russian Journal of Physical Chemistry A*, vol. 95, no. Suppl 1, pp. S44-S55, 2021. https://doi.org/10.1134/S0036024421140235

[27] M. D. Meti, S. T. Nandibewoor, and S. A. Chimatadar, "Oxidation of procainamide by diperiodatocuprate (III) complex in aqueous alkaline medium: A comparative kinetic study," *Inorganic and Nano-Metal Chemistry*, vol. 50, no. 4, pp. 195-204, 2020. https://doi.org/10.1080/24701556.2019.1662041

[28] C. Kathari, P. Pol, and S. T. Nandibewoor, "The kinetics and mechanism of oxidation of vanillin by diperiodatonickelate (IV) in aqueous alkaline medium," *Turkish Journal of Chemistry*, vol. 26, no. 2, pp. 229-236, 2002.

[29] Y. Zhao, M. Qi, R. Hao, J. Jiang, and B. Yuan, "A novel catalytic oxidation process for removing elemental mercury by using diperiodatoargentate (III) in the catalysis of trace ruthenium (III)," *Journal of Hazardous Materials*, vol. 381, p. 120964, 2020. https://doi.org/10.1016/j.jhazmat.2019.120964

[30] R. R. Hosamani, N. P. Shetti, and S. T. Nandibewoor, "Mechanistic investigation on the oxidation of ampicillin drug by diperiodatoargentate (III) in aqueous alkaline medium," *Journal of Physical Organic Chemistry*, vol. 22, no. 3, pp. 234-240, 2009. https://doi.org/10.1002/poc.1460

[31] S. Nadimpalli, J. Padmavathy, and K. K. Yusuff, "Determination of the nature of the diperiodatocuprate (III) species in aqueous alkaline medium through a kinetic and mechanistic study on the oxidation of iodide ion," *Transition Metal Chemistry*, vol. 26, pp. 315-321, 2001. https://doi.org/10.1023/A:1007116932047

[32] B. Chowdhury, M. H. Mondal, M. K. Barman, and B. Saha, "A study on the synthesis of alkaline copper (III)-periodate (DPC) complex with an overview of its redox behavior in aqueous micellar media," *Research on Chemical Intermediates*, vol. 45, pp. 789-800, 2019. https://doi.org/10.1007/S11164-018-3643-2

[33] W. Levason and M. D. Spicer, "The chemistry of copper and silver in their higher oxidation states," *Coordination Chemistry Reviews*, vol. 76, pp. 45-120, 1987. https://doi.org/10.1016/0010-8545(87)85002-6

[34] H.-Y. Xie, Z.-R. Wang, and Z.-F. Fu, "Highly sensitive trivalent copper chelate–luminol chemiluminescence system for capillary electrophoresis chiral separation and determination of ofloxacin enantiomers in urine samples," *Journal of Pharmaceutical Analysis*, vol. 4, no. 6, pp. 412-416, 2014. https://doi.org/10.1016/j.jpha.2014.05.004

[35] B. Sethuram, *Some aspects of electron transfer reaction involving organic molecules*. New Delhi: Allied Publishers Pvt. Ltd, 2003.

[36] L. Eberson, "Electron-transfer reactions in organic chemistry," *Advances in Physical Organic Chemistry*, vol. 18, pp. 79-185, 1982. https://doi.org/10.1016/S0065-3160(08)60139

[37] A. L. Giraldo, E. D. Erazo-Erazo, O. A. Flórez-Acosta, E. A. Serna-Galvis, and R. A. Torres-Palma, "Degradation of the antibiotic oxacillin in water by anodic oxidation with Ti/IrO2 anodes: Evaluation of degradation routes, organic by-products and effects of water matrix components," *Chemical Engineering Journal*, vol. 279, pp. 103-114, 2015. https://doi.org/10.1016/j.cej.2015.04.140

[38] E. Takács *et al.*, "Elimination of oxacillin, its toxicity and antibacterial activity by using ionizing radiation," *Chemosphere*, vol. 286, p. 131467, 2022. https://doi.org/10.1016/j.chemosphere.2021.131467

*Edelweiss Applied Science and Technology*
*ISSN: 2576-8484*
*Vol. 8, No. 3: 102-124, 2024*
*DOI: 10.55214/25768484.v8i3.1095*

[39] R. M. Moghadam, L. Salehi, S. Jafari, N. Nasirizadeh, and J. Ghasemi, "Voltammetric sensing of oxacillin by using a screen-printed electrode modified with molecularly imprinted polyaniline, gold nanourchins and graphene oxide," *Microchimica Acta*, vol. 186, pp. 1-7, 2019. https://doi.org/10.1007/s00604-019-3981-9

[40] A. F. Kaizal, J. M. Salman, and P. Kot, "Evaluation of some heavy metals, their fate and transportation in water, sediment, and some biota within Al-Musayyib River, Babylon Governorate, Iraq," *Baghdad Science Journal*, vol. 20, no. 2, pp. 0436-0436, 2023. http://dx.doi.org/10.21123/bsj.2022.7599

[41] M. Mohammadi Tabar, M. Khaleghi, E. Bidram, A. Zarepour, and A. Zarrabi, "Penicillin and oxacillin loaded on pegylated-graphene oxide to enhance the activity of the antibiotics against methicillin-resistant staphylococcus aureus," *Pharmaceutics*, vol. 14, p. 2049, 2022. https://doi.org/10.3390/pharmaceutics14102049

[42] S. M. Ibrahim, N. Saad, M. M. Ahmed, and M. Abd El–Aal, "Novel synthesis of antibacterial pyrone derivatives using kinetics and mechanism of oxidation of azithromycin by alkaline permanganate," *Bioorganic Chemistry*, vol. 119, p. 105553, 2022. https://doi.org/10.1016/j.bioorg.2021.105553

[43] M. M. Barbooti and S. H. Zahraw, "Removal of amoxicillin from water by adsorption on water treatment residues," *Baghdad Science Journal*, vol. 17, no. 3 (Suppl.), pp. 1071-1071, 2020. http://dx.doi.org/10.21123/bsj.2020.17.3(Suppl.).1071

[44] P. Jaiswal and K. Yadava, "Determination of sugars and organic acids with periodato complex of Cu (III)," *Chemischer Informationsdienst*, vol. 4, no. 51, pp. 837-838, 1973.

[45] G. H. Jeffery, J. Basset, R. C. Mendham, and R. C. Denney, *Vogel's textbook of qualitative chemical analysis*, 5th ed. Essex U. K: ELBS, Longman, 1996.

[46] G. Panigrahi and A. Pathy, "Kinetics and mechanism of oxidation of S 2 O 3 2− by potassium bis (tellurato) cuprate (III)," *Journal of Chemical Sciences*, vol. 96, pp. 301-308, 1986. https://doi.org/10.1007/bf02895725

[47] J. S. Renny, L. L. Tomasevich, E. H. Tallmadge, and D. B. Collum, "Method of continuous variations: Applications of job plots to the study of molecular associations in organometallic chemistry," *Angewandte Chemie International Edition*, vol. 52, no. 46, pp. 11998-12013, 2013. https://doi.org/10.1002/anie.201304157

[48] E. Coşkun, E. Duman, N. Acar, and E. Biçer, "Electrochemical, spectroscopic and computational studies on complexation of oxacillin with Cu (II) and Co (II) ions. Synthesis and ligand hydrolysis," *International Journal of Electrochemical Science*, vol. 12, no. 10, pp. 9364-9377, 2017. https://doi.org/10.20964/2017.10.43

[49] S. Ramotowska, M. Wysocka, J. Brzeski, A. Chylewska, and M. Makowski, "A comprehensive approach to the analysis of antibiotic-metal complexes," *TrAC Trends in Analytical Chemistry*, vol. 123, p. 115771, 2020. https://doi.org/10.1016/j.trac.2019.115771

*Edelweiss Applied Science and Technology*
*ISSN: 2576-8484*
*Vol. 8, No. 3: 102-124, 2024*
*DOI: 10.55214/25768484.v8i3.1095*

## Appendix

FT-IR and LC-MS spectral evidence have been represented herein as Figures A1 and A2.

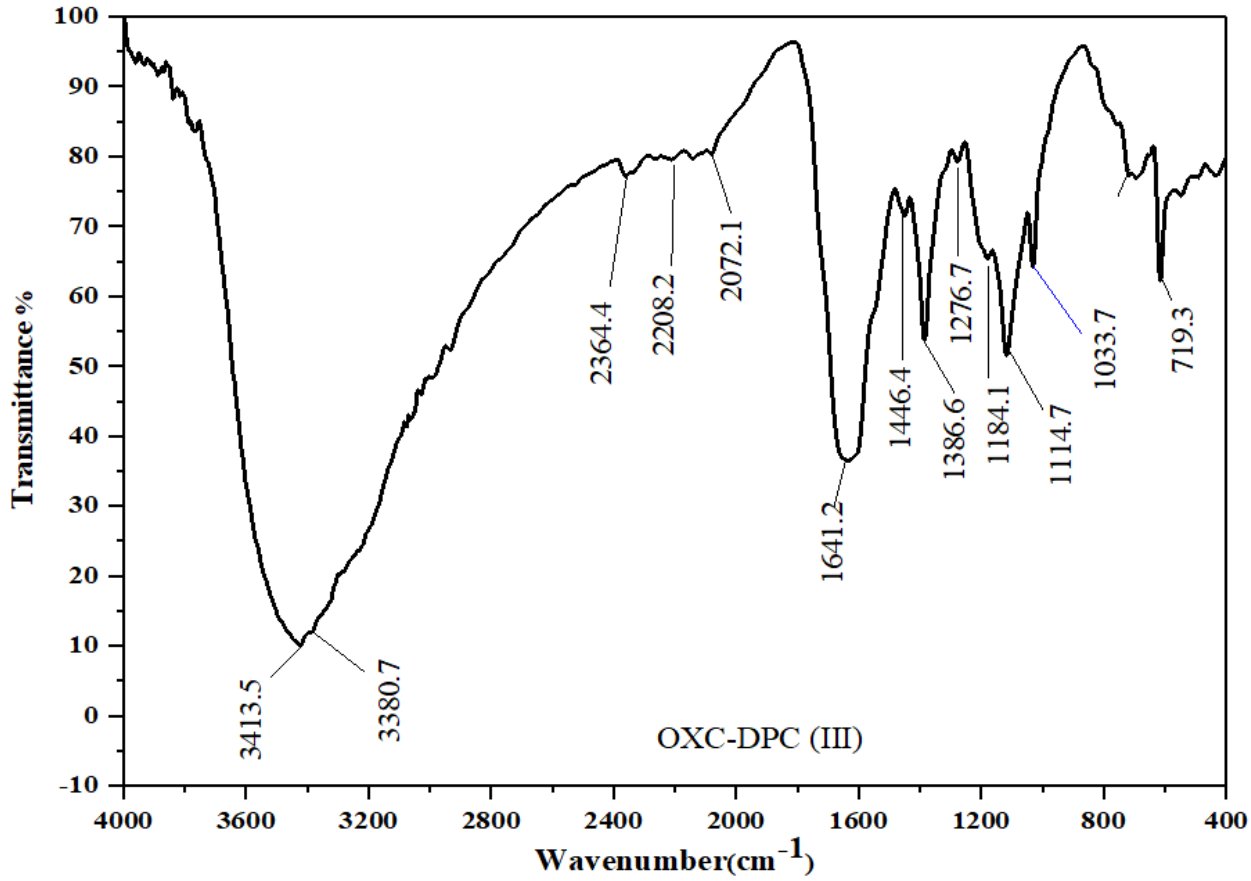


**Figure A1.**
Displays the oxacillin oxidation by DPC (III): FT-IR spectrum.

*Edelweiss Applied Science and Technology*
*ISSN: 2576-8484*
*Vol. 8, No. 3: 102-124, 2024*
*DOI: 10.55214/25768484.v8i3.1095*

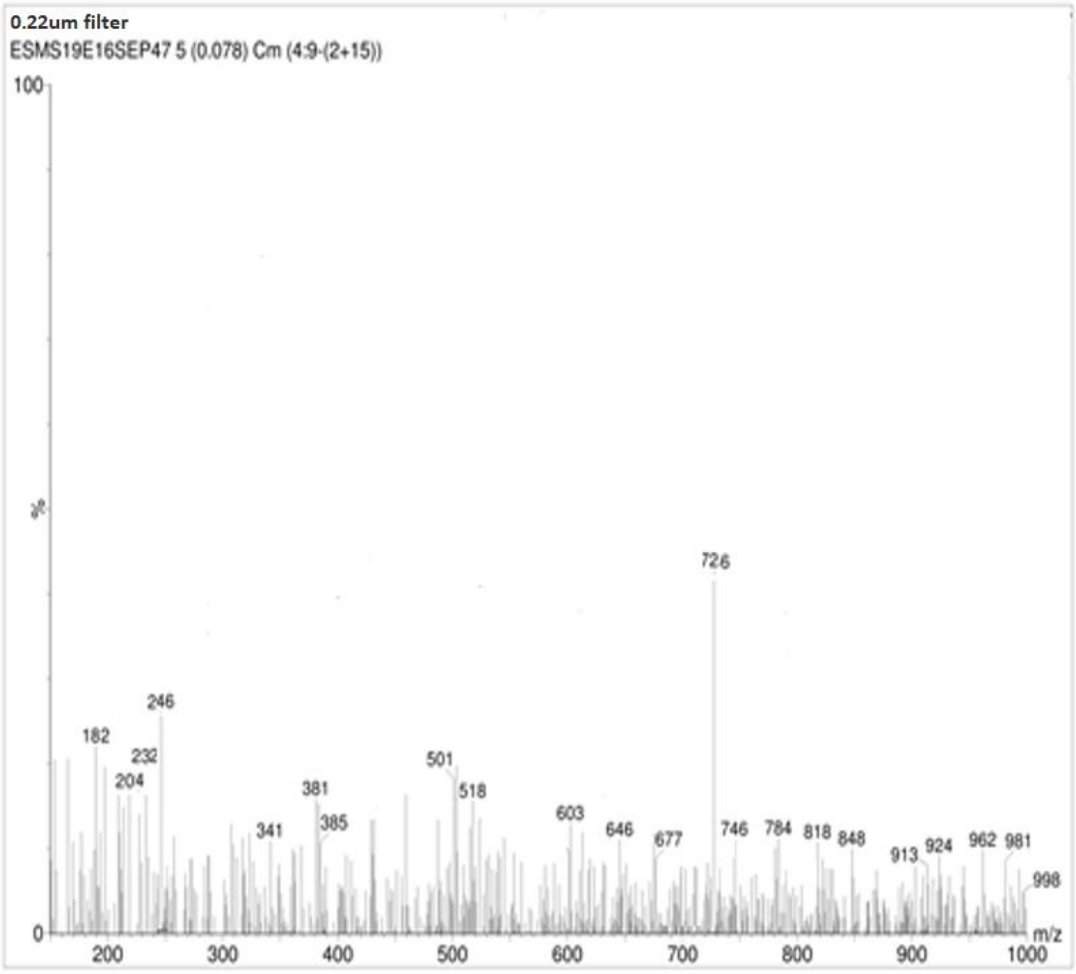


**Figure A2.**
Displays the LC-MS spectrum of the OXC-MPC (III) complex and its products.

*Edelweiss Applied Science and Technology*
*ISSN: 2576-8484*
*Vol. 8, No. 3: 102-124, 2024*
*DOI: 10.55214/25768484.v8i3.1095*